

Using matrix projection model to predict climate-induced range expansion/contraction for a dioecious range-limited species

Jacob K. Moutouama¹, Aldo Compagnoni², and Tom E.X. Miller¹

¹Program in Ecology and Evolutionary Biology, Department of BioSciences, Rice University, Houston, TX USA

²Institute of Biology, Martin Luther University Halle-Wittenberg, Halle, Germany; and German Centre for Integrative Biodiversity Research (iDiv), Leipzig, Germany

December 3, 2023

* Corresponding author: jmoutouama@gmail.com

Submitted to *Ecological Monographs*

Manuscript type: Article

Open Research statement: All of our data and code are available during peer review at <https://github.com/jmoutouama/POAR-Forecasting>. This manuscript and its contents can be reproduced from this file: <https://github.com/jmoutouama/POAR-Forecasting/Manuscript/Forescasting.Rnw>. All data are provided at <https://github.com/jmoutouama/POAR-Forecasting/tree/main/data>.

1

Abstract

2

Keywords

2

Introduction

Rising temperatures and extreme drought events associated with global climate change are leading to increased concern about how species will become redistributed across the globe under future climate conditions (Bertrand et al., 2011; Gamelon et al., 2017). Dioecious species might be particularly vulnerable to the influence of climate change because they often display skewed sex ratios that are generated or reinforced by sexual niche differentiation (distinct responses of females and males to shared climate drivers) (Tognetti, 2012). Accounting for such a niche differentiation between male and female within a population is a long-standing challenge in accurately predicting which sex will successfully track environmental change and how this will impact population dynamics (Jones et al., 1999; Gissi et al., 2023a). The vast majority of theory and models in population biology, including those used to forecast biodiversity responses to climate change, ignore the complication of sex structure (Pottier et al., 2021; Ellis et al., 2017). As a result, accurate forecasts of colonization-extinction dynamics for dioecious species under future climate scenarios are limited.

Females and males respond differently to climate change, especially in species where there is sexual niche differentiation (Gissi et al., 2023a,b; Hultine et al., 2016). This sex-specific response to climate change may help one sex to succeed in extreme climatic conditions rather than the other sex (Zhao et al., 2012; Bürli et al., 2022) leading to a skewness in the operational sex ratio (relative number of males and females who are ready to mate) (Eberhart-Phillips et al., 2017) . Experimentation manipulation revealed that when exposed to increasing temperatures, for example, in two populations of Atlantic marine copepods (*Acartia tonsa*), males showed significantly lower survival than females (Sasaki et al., 2019). However, in some species, such as *Pteropus poliocephalus* or

27 *Populus cathayana*, females showed lower survival than males in response to high tem-
28 perature (Welbergen et al., 2008; Zhao et al., 2012).

29 The geographic range of most species may be limited by climatic factors, including
30 temperature, precipitation. Any substantial changes in the magnitude of these climatic
31 factors in a given location could impact species population viability, with potential impli-
32 cation on range shift (Davis and Shaw, 2001; Pease et al., 1989). This is particularly true
33 for dioecious species in which each sex has a different sensitivity to climate variation.
34 Populations in which males are rare under current climatic conditions could experience
35 low reproductive success due to sperm or pollen limitation that may lead to population
36 decline in response to climate change (Eberhart-Phillips et al., 2017). In contrast, climate
37 change could lead to male moving to more suitable areas (e.g. upslope), which might
38 reduce pollen limitation, increases seedset and favor range expansion (Petry et al., 2016).
39 Although the response of species to warming is generally understood, it is difficult to
40 disentangle the interaction between sex and climate drivers to understand their relative
41 contribution and effect on population dynamics and the consequence of such effect on
42 range shift.

43 Our ability to track the impact of climate change on the population dynamics of
44 dioecious plants and the implication of such impact on range shift depends on our ability
45 to build mechanistic models that take into account the spatial and temporal context in
46 which sex specific response to climate change affects population viability (Davis and
47 Shaw, 2001; Evans et al., 2016; Czachura and Miller, 2020). At their range edge where
48 climatic conditions are expected to be less favorable, if dioecious species populations are
49 non-viable in response to climate change, global warming will induce range contraction
50 in dioecious species. In reverse, if populations at the edge are viable habitats in response
51 to global warming, dioecious species populations could shift their range and relocate to

52 more favorable and thereby favored range expansion.

53 In this study, we used a mechanistic approach by combining field experiment and ma-
54 trix projection modelling, to understand the demographic response of dioecious species
55 to climate change and its implications for future range dynamics. Our study system
56 is a dioecious plant species (*Poa arachnifera*) distributed along environmental gradients
57 in the south-central US corresponding to variation in temperature across latitude and
58 precipitation across longitude (MAP). Here, we asked three questions: (1) What is the
59 sex-specific demographic response to rising temperature and precipitation ? (2) How
60 that sex-specific demographic response affects populations dynamics under current and
61 future climatic conditions ? (3) What are the implications of population dynamics on
62 range dynamics ?

63 Materials and methods

64 *Study species*

65 Texas bluegrass (*Poa arachnifera*) is a perennial, summer-dormant cool-season (C3) grass.
66 The species occurs in Texas, Oklahoma, and southern Kansas, USA (Hitchcock, 1971).
67 Texas bluegrass grows during cool months between October and May, with onset of
68 dormancy often from June to September (Kindiger, 2004). Flowering occurs in May and
69 the species is pollinated by wind (Hitchcock, 1971).

70 *Common garden experiment*

71 We set up a common garden experiment to manipulate climatic factors (e.g.,temperature
72 and precipitation) to detect mechanisms underlying sex-specific demographic response
73 to climate and the implication of such a response on range limitation (Merow et al.,

74 2017; Schwinning et al., 2022). At this end, we collected vegetative tillers from flower-
75 ing individuals of each sex in eight natural (sources) populations of the focal species.
76 We then propagated these tillers in ProMix plotting soil and supplemented them with
77 Osmocote slow-release fertilizer at 75°F to 85°F under natural climatic conditions at the
78 Rice University Greenhouse. The common experiment was installed on 14 sites across
79 a precipitation gradient (FigX). At each site, we established 14 blocks. Each block was
80 selected so that they resemble the natural environment of the species. For each block we
81 planted three females and three males individuals. We spared the individuals, provided
82 1 L of water, and removed surrounding vegetation to avoid competition and promote
83 establishment.

84 *Demographic and climatic data collection*

85 To parametrize the demographic models, we first collected individual demographic data
86 including survival (alive or dead), growth (number of tillers), flowers (reproductive or
87 vegetative), and fertility (number of panicles) in each site for two censuses (2015 and
88 2016). Secondly, we downloaded monthly temperature and precipitation from Chelsa to
89 describe current (2015–2016) climate conditions (Karger et al., 2017). These climate data
90 were used as covariates in vital rate regressions, which allowed us to forecast and back
91 cast the effect of climate change on population dynamics and map species' distributions
92 under future and past climate change. We prefer temperature and precipitation because
93 they capture the most the climate in the study region. Since our experiment was installed
94 in November, we aligned the climatic years to match demographic transition years rather
95 than calendar years. Then we used the monthly data to estimate seasonal data (dormant
96 and growing season), since our study species is a seasonal cool grass. We define June
97 to September as the dormant season of the year and the rest of the year as the growing

98 season. To forecast the effect of future climate on species population dynamics, we
99 downloaded climatic projection data (2017-20100) from four general circulation models
100 (GCMs) selected from the Coupled Model Intercomparison Project Phase 5 (CMIP5).
101 These GCMs are MIROC5, ACCESS1-3, CESM1-BGC, CMCC-CM and were downloaded
102 from chelsa (Sanderson et al., 2015). We evaluated future climate projections from two
103 scenarios of representative concentration pathways (RCPs): RCP4.5, an intermediate-to-
104 pessimistic scenario assuming a radiative forcing to amount to 4.5 Wm^{-2} by 2100, and
105 RCP8.5, a pessimistic emission scenario which project a radiative forcing to amount to
106 8.5 Wm^{-2} by 2100 (Thomson et al., 2011; Schwalm et al., 2020).

107 *Sex ratio experiment*

108 We¹ also conducted a sex-ratio experiment to measure the effect of male panicle avail-
109 ability on seed viability on females panicles. Details of the experiment are provided in
110 Compagnoni et al. (2017) and Miller and Compagnoni (2022).²

111 We used the sex-ratio to estimate the probability of viability and the germination
112 rate. Seed viability was modeled with a binomial distribution where the probability of
113 viability (v) was given by:

$$v = v_0 * (1 - OSR^\alpha) \quad (1)$$

114 where OSR is the operational sex ratio³ (proportion of panicles that were female) in
115 the experimental populations. The properties of the above function is supported by our
116 previous work (Compagnoni et al., 2017). Here, seed viability is maximized at v_0 as OSR

¹I would describe the demographic data before the sex ratio experiment.

²Again, you need more info here.

³This concept should be described in the Introduction.

117 approaches zero (strongly male-biased) and goes to zero as OSR approaches 1 (strongly
118 female-biased). Parameter α controls how viability declines with increasing female bias.

119 We used a binomial distribution to model the germination data from greenhouse
120 trials. Given that germination was conditional on seed viability, the probability of success
121 was given by the product $v * g$, where v is a function of OSR (Eq. 1) and g is assumed to
122 be constant.

123 *Vital rate responses to climate*

124 We used individual level measurements of survival, growth (number of tillers), flow-
125 ering, number of panicles to independently develop Bayesian mixed effect models de-
126 scribing how each vital rate varies as a function of sex, size, precipitation of growing and
127 dormant season and temperature of of growing and dormant season. We fit two versions
128 of the vital rate models, with either linear or second-degree polynomial functions for the
129 influence of climate, and used model selection to quantify their empirical support. We
130 included a second-degree polynomial because we expected that climate variables would
131 affect vital rates through a hump-shaped relationship.

132 We centered and standardized all predictors to facilitate model convergence. We
133 included site, **source, and block**⁴ as random effect. All the vital rate models used the
134 same **linear and quadratic predictor**⁵ for the expected value (μ). However, we applied
135 a different link function ($f(\mu)$) depending on the distribution the vital rate ([Appendix](#)
136 [S1: Section S1](#)). We modeled survival and flowering data with a Bernoulli distribution.
137 We modeled the growth (tiller number) with a zero-truncated Poisson inverse Gaussian
138 distribution. Fertility (panicle count) was model as zero-truncated negative binomial. We
139 fit all models in Stan (Stan Development Team, 2023), with weakly informative priors for

⁴*You have not described these.*

⁵*show these*

140 coefficients ($\mu = 0, \sigma = 100$) and variances ($\gamma[0.001, 0.001]$). We ran three chains for 1000
141 samples for warmup and 40000 for interactions, with a thinning rate of 3. We accessed
142 the quality of the models using trace plots and predictive check graphs (Piironen and
143 Vehtari, 2017) (Appendix S1: Figure S1). Then, we used approximate Bayesian leave-
144 one-out cross-validation (LOOIC) to select the best model describing the effect of climate
145 variable on vital rate. The final model was the model with the lowest LOOIC (Vehtari
146 et al., 2017).

147 To understand the effect of climate on vital rates, we used the 95 % credible interval
148 of the final model for each vital rate. When the 95 % credible interval of the coefficient
149 of a given climatic variable did not include zero, we concluded that there is a strong
150 effect of that variable on the vital rate. In contrast, when we have a credible interval of
151 a climatic variable that includes zero, we used the empirical cumulative distribution to
152 find the probability that the coefficient of that climatic variable is greater than zero.⁶

153 *Population growth rate responses to climate*

154 To understand the effect of climate on population growth rate, we used the vital rate
155 estimated earlier to build a matrix projection model (MPM) structured by size (number
156 of tillers) and sex with "Climate"⁷ as covariate. For a given climatic variable⁸, let $F_{x,t}$ and
157 $M_{x,t}$ be the number of female and male plants of size x in year t , where $x \in \{1, 2, \dots, U\}$
158 and U is the maximum number of tillers a plant can reach (here 99th percentile of ob-
159 served maximum size). Let F_t^R and M_t^R be the new recruits, which we assume do not
160 reproduce in their first year. We assume that the parameters of sex ratio-dependent mat-

⁶I would prefer to not interpret the coefficient posteriors in this way, because it is effectively frequentist hypothesis-testing.

⁷why quotes?

⁸I am not sure why this is conditional on a climate variable. I think you are suggesting that this model applies to a specific level of climate values. However, I think you should instead modify the notation of the model so that it is explicitly climate-dependent, eg $F_{x,c,t}$

¹⁶¹ ing (Eq. 1) do not vary with climate. For a pre-breeding census, the expected numbers
¹⁶² of recruits in year $t + 1$ is given by:

$$F_{t+1}^R = \sum_{x=1}^U [p^F(x) \cdot c^F(x) \cdot d \cdot v(\mathbf{F}_t, \mathbf{M}_t) \cdot m \cdot \rho] F_{x,t} \quad (2)$$

$$M_{t+1}^R = \sum_{x=1}^U [p^F(x) \cdot c^F(x) \cdot d \cdot v(\mathbf{F}_t, \mathbf{M}_t) \cdot m \cdot (1 - \rho)] F_{x,t} \quad (3)$$

¹⁶³ where p^F and c^F are flowering probability and panicle production for females of size x ,
¹⁶⁴ d is the number of seeds per female panicle, v is the probability that a seed is fertilized,
¹⁶⁵ m is the probability that a fertilized seed germinates, and ρ is the primary sex ratio
¹⁶⁶ (proportion of recruits that are female). Seed fertilization depends on the OSR of panicles
¹⁶⁷ (following Eq. 1) which was derived from the $U \times 1$ vectors of population structure \mathbf{F}_t
¹⁶⁸ and \mathbf{M}_t :

$$v(\mathbf{F}_t, \mathbf{M}_t) = v_0 * \left[1 - \left(\frac{\sum_{x=1}^U p^F(x) c^F(x) F_{x,t}}{\sum_{x=1}^U p^F(x) c^F(x) F_{x,t} + p^M(x) c^M(x) M_{x,t}} \right)^\alpha \right] \quad (4)$$

¹⁶⁹ Thus, the dynamics of the size-structured component of the population are given by:

$$F_{y,t+1} = [\sigma \cdot g^F(y, x = 1)] F_t^R + \sum_{x=1}^U [s^F(x) \cdot g^F(y, x)] F_{x,t} \quad (5)$$

$$M_{y,t+1} = [\sigma \cdot g^M(y, x = 1)] M_t^R + \sum_{x=1}^U [s^M(x) \cdot g^M(y, x)] M_{x,t} \quad (6)$$

¹⁷⁰ In the two formula above, the first term represents seedlings that survived their first
¹⁷¹ year and enter the size distribution of established plants. Instead of using *P. arachnifera*
¹⁷² survival probability, we used the seedling survival probability (σ) from demographic
¹⁷³ studies of the hermaphroditic congener *Poa autumnalis* in east Texas (T.E.X. Miller and
¹⁷⁴ J.A. Rudgers, *unpublished data*), and we assume this probability was constant across sexes

and climatic variables. We did this because we had little information on the early life cycle transitions of **greenhouse-raised transplants**⁹. We also assume that $g(y, x = 1)$ is the probability that a surviving seedlings reach size y , the expected future size of 1-tiller plants from the transplant experiment. The second term represents survival and size transition of established plants from the previous year, where s and g give the probabilities of surviving at size x and growing from sizes x to y , respectively, and superscripts indicate that these functions may be unique to females (F) and males (M).

Because the two-sex MPM is nonlinear (vital rates affect and are affected by population structure) we estimated the asymptotic geometric growth rate (λ) by numerical simulation, and repeated this across a range of climate.

Identifying the mechanisms of population growth rate sensitivity to climate

To identify the mechanism by which climate affects population growth rate, we decomposed the effect of each climate variable (here Climate) on population growth rate (λ) into contribution arising from the effect on each stage-specific vital rate (Caswell, 2000). At this end we used a life table response experiment (LTRE) with a regression designs. The LTRE approximates the change in λ with climate as the product of the sensitivity of λ to the parameters times the sensitivity of the parameters to climate, summed over all parameters (Caswell, 1989):

$$\frac{\partial \lambda}{\partial \text{Climate}} \approx \sum_i \frac{\partial \lambda}{\partial \theta_i^F} \frac{\partial \theta_i^F}{\partial \text{Climate}} + \frac{\partial \lambda}{\partial \theta_i^M} \frac{\partial \theta_i^M}{\partial \text{Climate}} \quad (7)$$

where, θ_i^F and θ_i^M represent sex-specific parameters: the regression coefficients for the

⁹You have not described these.

¹⁰I don't think the LTRE analysis is adequately motivated by the Intro.

195 intercepts and slopes of size-dependent vital rate functions. Because LTRE contributions
196 are additive, we summed across vital rates to compare the total contributions of female
197 and male parameters.

198 *Implication on niche breath and range expansion/contraction*

199 To understand the implication of our study on **niche breath**¹¹, we projected the popula-
200 tion growth current and future prediction on two axes of climatic conditions (tempera-
201 ture and precipitation) of each seasonal season (dormant and growing season). Similarly,
202 to understand the implication of our study on range contraction on expansion, we extrap-
203 olate population growth current and future prediction across the range to map species
204 distributions.

205 All the analysis were performed in R 4.3.1 (R Core Team, 2023)

¹¹*You have not defined this, or described how it relates to geographic ranges.*

Appendix S1

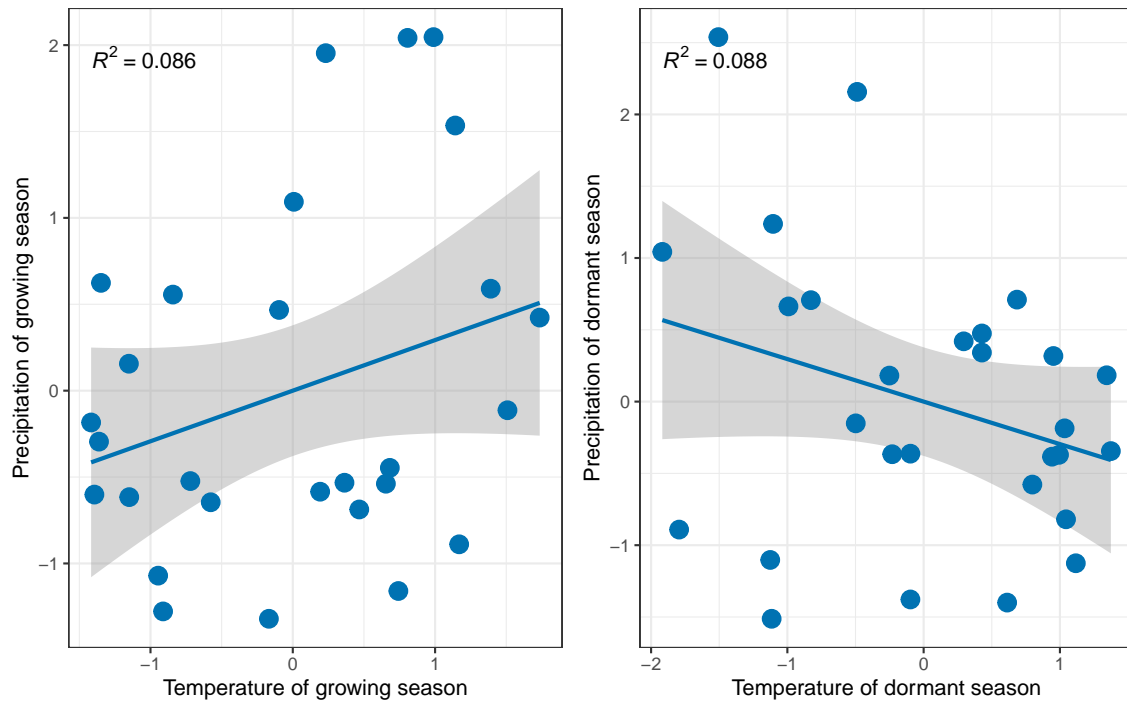


Figure S1: Relation between precipitation and temperature for each season (growing and dormant). R^2 indicates the value of proportion of explained variance between the temperature and precipitation

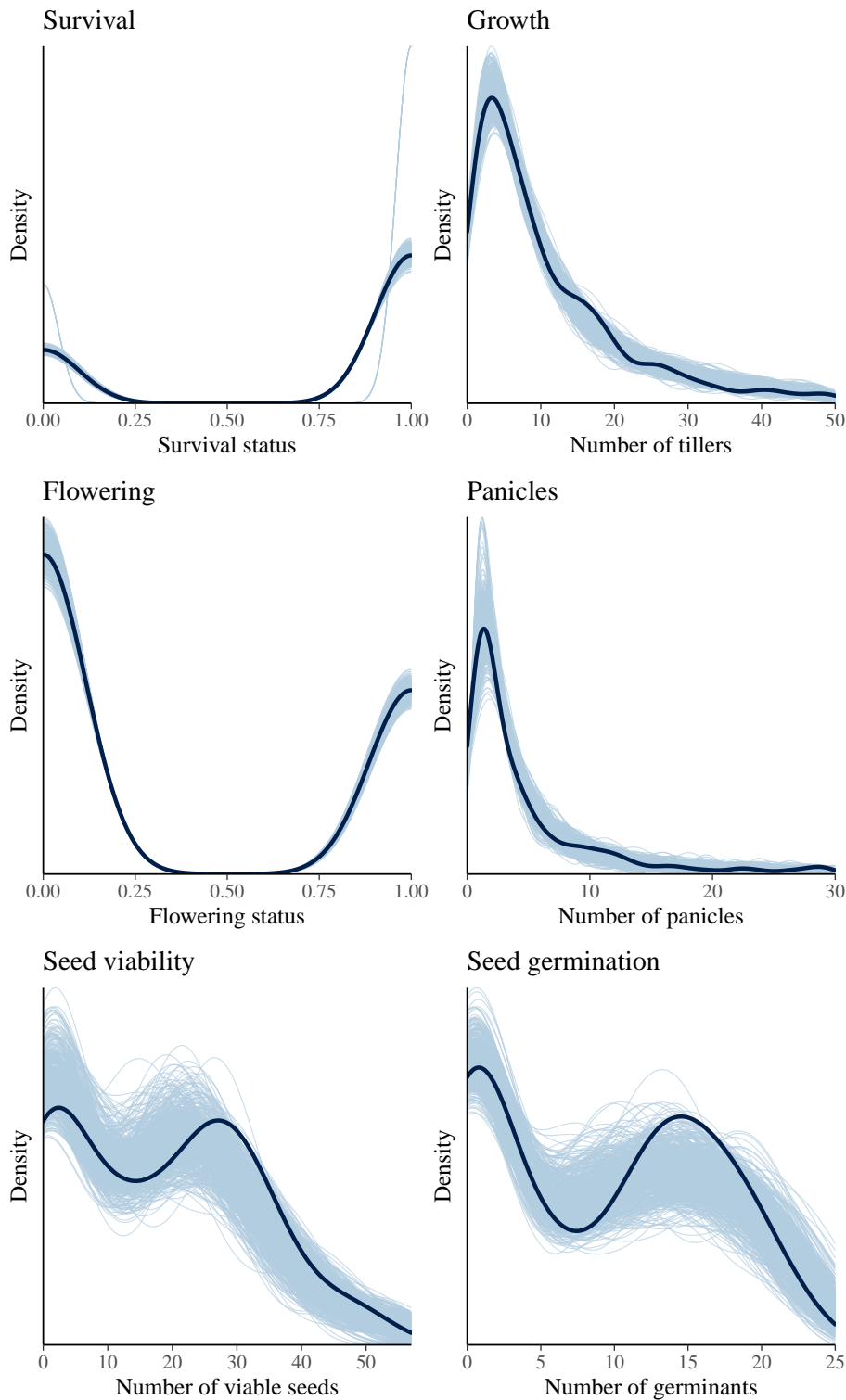


Figure S2: Consistency between real data and simulated values suggests that the fitted model accurately describes the data. Graph shows density curves for the observed data (light blue) along with the simulated values (dark blue). The first column shows the linear models and the second column shows the 2 degree polynomial models.

Section S1

$$S \sim Bernoulli(\hat{S}) \quad (1a)$$

$$F \sim Bernoulli(\hat{F}) \quad (1b)$$

$$G \sim Zero-truncated Poisson inverse Gaussian(\hat{G}) \quad (1c)$$

$$Fer \sim Zero-truncated negative binomial(\hat{Fer}) \quad (1d)$$

$$\hat{S} = \frac{\exp(f(\mu))}{1 + \exp(f(\mu))} \quad (2a)$$

$$\hat{F} = \frac{\exp(f(\mu))}{1 + \exp(f(\mu))} \quad (2b)$$

$$\hat{G} = \exp(f(\mu)) \quad (2c)$$

$$\hat{Fer} = \exp(f(\mu)) \quad (2d)$$

$$\begin{aligned}
f(\mu) = & \beta_0 + \beta_1 size + \beta_2 sex + \beta_3 pptgrow + \beta_4 pptdorm + \beta_5 tempgrow \\
& + \beta_6 tempdorm + \beta_7 pptgrow * sex + \beta_8 pptdorm * sex + \beta_9 tempgrow * sex \\
& + \beta_{10} tempdorm * sex + \beta_{11} size * sex + \beta_{12} pptgrow * tempgrow \\
& + \beta_{13} pptdorm * tempdorm + \beta_{14} pptgrow * tempgrow * sex \\
& + \beta_{15} pptdorm * tempdorm * sex + \beta_{16} pptgrow^2 + \beta_{17} pptdorm^2 \\
& + \beta_{18} tempgrow^2 + \beta_{19} tempdorm^2 + \beta_{20} pptgrow^2 * sex \\
& + \beta_{21} pptdorm^2 * sex + \beta_{22} tempgrow^2 * sex \\
& + \beta_{23} tempdorm^2 * sex + \phi + \rho + \nu
\end{aligned} \tag{3}$$

210

Literature Cited

- 211 Bertrand, R., J. Lenoir, C. Piedallu, G. Riofrío-Dillon, P. De Ruffray, C. Vidal, J.-C. Pierrat,
212 and J.-C. Gégout. 2011. Changes in plant community composition lag behind climate
213 warming in lowland forests. *Nature* **479**:517–520.
- 214 Bürli, S., J. R. Pannell, and J. Tonnabel. 2022. Environmental variation in sex ra-
215 tios and sexual dimorphism in three wind-pollinated dioecious plant species. *Oikos*
216 **2022**:e08651.
- 217 Caswell, H. 1989. Analysis of life table response experiments I. Decomposition of effects
218 on population growth rate. *Ecological Modelling* **46**:221–237.
- 219 Caswell, H. 2000. Matrix population models. Sinauer Sunderland, MA.
- 220 Compagnoni, A., K. Steigman, and T. E. Miller. 2017. Can't live with them, can't live
221 without them? Balancing mating and competition in two-sex populations. *Proceedings*
222 of the Royal Society B: Biological Sciences **284**:20171999.
- 223 Czachura, K., and T. E. Miller. 2020. Demographic back-casting reveals that subtle
224 dimensions of climate change have strong effects on population viability. *Journal of*
225 *Ecology* **108**:2557–2570.
- 226 Davis, M. B., and R. G. Shaw. 2001. Range shifts and adaptive responses to Quaternary
227 climate change. *Science* **292**:673–679.
- 228 Eberhart-Phillips, L. J., C. Küpper, T. E. Miller, M. Cruz-López, K. H. Maher,
229 N. Dos Remedios, M. A. Stoffel, J. I. Hoffman, O. Krüger, and T. Székely. 2017. Sex-
230 specific early survival drives adult sex ratio bias in snowy plovers and impacts mating

- 231 system and population growth. *Proceedings of the National Academy of Sciences*
232 **114**:E5474–E5481.
- 233 Ellis, R. P., W. Davison, A. M. Queirós, K. J. Kroeker, P. Calosi, S. Dupont, J. I. Spicer, R. W.
234 Wilson, S. Widdicombe, and M. A. Urbina. 2017. Does sex really matter? Explaining
235 intraspecies variation in ocean acidification responses. *Biology letters* **13**:20160761.
- 236 Evans, M. E., C. Merow, S. Record, S. M. McMahon, and B. J. Enquist. 2016. Towards
237 process-based range modeling of many species. *Trends in Ecology & Evolution* **31**:860–
238 871.
- 239 Gamelon, M., V. Grøtan, A. L. Nilsson, S. Engen, J. W. Hurrell, K. Jerstad, A. S. Phillips,
240 O. W. Røstad, T. Slagsvold, B. Walseng, et al. 2017. Interactions between demogra-
241 phy and environmental effects are important determinants of population dynamics.
242 *Science Advances* **3**:e1602298.
- 243 Gissi, E., L. Schiebinger, E. A. Hadly, L. B. Crowder, R. Santolieri, and F. Micheli. 2023a.
244 Exploring climate-induced sex-based differences in aquatic and terrestrial ecosystems
245 to mitigate biodiversity loss. *nature communications* **14**:4787.
- 246 Gissi, E., L. Schiebinger, R. Santolieri, and F. Micheli. 2023b. Sex analysis in marine bio-
247 logical systems: insights and opportunities. *Frontiers in Ecology and the Environment*
248 .
- 249 Hitchcock, A. S. 1971. *Manual of the grasses of the United States*. Courier Corporation.
- 250 Hultine, K. R., K. C. Grady, T. E. Wood, S. M. Shuster, J. C. Stella, and T. G. Whitham.
251 2016. Climate change perils for dioecious plant species. *Nature Plants* **2**:1–8.
- 252 Jones, M. H., S. E. Macdonald, and G. H. Henry. 1999. Sex-and habitat-specific responses

- 253 of a high arctic willow, *Salix arctica*, to experimental climate change. *Oikos* pages
254 129–138.
- 255 Karger, D. N., O. Conrad, J. Böhner, T. Kawohl, H. Kreft, R. W. Soria-Auza, N. E. Zim-
256 mermann, H. P. Linder, and M. Kessler. 2017. Climatologies at high resolution for the
257 earth's land surface areas. *Scientific data* **4**:1–20.
- 258 Kindiger, B. 2004. Interspecific hybrids of *Poa arachnifera* × *Poa secunda*. *Journal of*
259 *New Seeds* **6**:1–26.
- 260 Merow, C., S. T. Bois, J. M. Allen, Y. Xie, and J. A. Silander Jr. 2017. Climate change
261 both facilitates and inhibits invasive plant ranges in New England. *Proceedings of the*
262 *National Academy of Sciences* **114**:E3276–E3284.
- 263 Miller, T. E., and A. Compagnoni. 2022. Two-Sex Demography, Sexual Niche Differen-
264 tiation, and the Geographic Range Limits of Texas Bluegrass (*Poa arachnifera*). *The*
265 *American Naturalist* **200**:17–31.
- 266 Pease, C. M., R. Lande, and J. Bull. 1989. A model of population growth, dispersal and
267 evolution in a changing environment. *Ecology* **70**:1657–1664.
- 268 Petry, W. K., J. D. Soule, A. M. Iler, A. Chicas-Mosier, D. W. Inouye, T. E. Miller, and K. A.
269 Mooney. 2016. Sex-specific responses to climate change in plants alter population sex
270 ratio and performance. *Science* **353**:69–71.
- 271 Piironen, J., and A. Vehtari. 2017. Comparison of Bayesian predictive methods for model
272 selection. *Statistics and Computing* **27**:711–735.
- 273 Pottier, P., S. Burke, S. M. Drobniaik, M. Lagisz, and S. Nakagawa. 2021. Sexual (in)
274 equality? A meta-analysis of sex differences in thermal acclimation capacity across
275 ectotherms. *Functional Ecology* **35**:2663–2678.

- 276 R Core Team. 2023. R: A Language and Environment for Statistical Computing. R
277 Foundation for Statistical Computing, Vienna, Austria. URL <https://www.R-project.org/>.
- 278
- 279 Sanderson, B. M., R. Knutti, and P. Caldwell. 2015. A representative democracy to reduce
280 interdependency in a multimodel ensemble. *Journal of Climate* **28**:5171–5194.
- 281 Sasaki, M., S. Hedberg, K. Richardson, and H. G. Dam. 2019. Complex interactions
282 between local adaptation, phenotypic plasticity and sex affect vulnerability to warming
283 in a widespread marine copepod. *Royal Society open science* **6**:182115.
- 284 Schwalm, C. R., S. Glendon, and P. B. Duffy. 2020. RCP8. 5 tracks cumulative CO₂
285 emissions. *Proceedings of the National Academy of Sciences* **117**:19656–19657.
- 286 Schwinning, S., C. J. Lortie, T. C. Esque, and L. A. DeFalco, 2022. What common-garden
287 experiments tell us about climate responses in plants.
- 288 Stan Development Team. 2023. RStan: the R interface to Stan. URL <https://mc-stan.org/>.
- 289
- 290 Thomson, A. M., K. V. Calvin, S. J. Smith, G. P. Kyle, A. Volke, P. Patel, S. Delgado-Arias,
291 B. Bond-Lamberty, M. A. Wise, L. E. Clarke, et al. 2011. RCP4. 5: a pathway for
292 stabilization of radiative forcing by 2100. *Climatic change* **109**:77–94.
- 293 Tognetti, R. 2012. Adaptation to climate change of dioecious plants: does gender balance
294 matter? *Tree Physiology* **32**:1321–1324. URL <https://doi.org/10.1093/treephys/tps105>.
- 295
- 296 Vehtari, A., A. Gelman, and J. Gabry. 2017. Practical Bayesian model evaluation using
297 leave-one-out cross-validation and WAIC. *Statistics and computing* **27**:1413–1432.

- 298 Welbergen, J. A., S. M. Klose, N. Markus, and P. Eby. 2008. Climate change and the
299 effects of temperature extremes on Australian flying-foxes. Proceedings of the Royal
300 Society B: Biological Sciences **275**:419–425.
- 301 Zhao, H., Y. Li, X. Zhang, H. Korpelainen, and C. Li. 2012. Sex-related and stage-
302 dependent source-to-sink transition in *Populus cathayana* grown at elevated CO₂ and
303 elevated temperature. Tree Physiology **32**:1325–1338.